



# Adsorption and binding dynamics of graphene-supported phospholipid membranes using the QCM-D technique

DOI:  
[10.1039/C7NR05639G](https://doi.org/10.1039/C7NR05639G)

**Document Version**  
Accepted author manuscript

[Link to publication record in Manchester Research Explorer](#)

## Citation for published version (APA):

Meléndrez Armada, D., Jowitt, T., Iliut, M., Verre, A. F., Goodwin, S., & Vijayaraghavan, A. (2018). Adsorption and binding dynamics of graphene-supported phospholipid membranes using the QCM-D technique. *Nanoscale*.  
<https://doi.org/10.1039/C7NR05639G>

**Published in:**  
Nanoscale

## Citing this paper

Please note that where the full-text provided on Manchester Research Explorer is the Author Accepted Manuscript or Proof version this may differ from the final Published version. If citing, it is advised that you check and use the publisher's definitive version.

## General rights

Copyright and moral rights for the publications made accessible in the Research Explorer are retained by the authors and/or other copyright owners and it is a condition of accessing publications that users recognise and abide by the legal requirements associated with these rights.

## Takedown policy

If you believe that this document breaches copyright please refer to the University of Manchester's Takedown Procedures [<http://man.ac.uk/04Y6Bo>] or contact [uml.scholarlycommunications@manchester.ac.uk](mailto:uml.scholarlycommunications@manchester.ac.uk) providing relevant details, so we can investigate your claim.



# Adsorption and binding dynamics of graphene-supported phospholipid membranes using the QCM-D technique

D. A. Melendrez<sup>a</sup>, T. Jowitt<sup>b</sup>, M. Iliut<sup>a</sup>, A.F. Verre<sup>a</sup>, S. Goodwin<sup>c</sup> and A. Vijayaraghavan<sup>†a,c</sup>

Received 00th January 20xx,  
Accepted 00th January 20xx

DOI: 10.1039/x0xx00000x

www.rsc.org/

We report on the adsorption dynamics of phospholipid membranes on graphene-coated substrates using the quartz crystal microbalance with dissipation monitoring (QCM-D) technique. We compare the lipid vesicle interaction and membrane formation on gold and silicon dioxide QCM crystal surfaces with their graphene oxide (GO) and reduced (r)GO coated counterparts, and report on the different lipid structures obtained. We establish graphene derivative coatings as support surfaces with tuneable hydrophobicity for the formation of controllable lipid structures. One structure of interest formed are lipid monolayer membranes which were formed on rGO, which are otherwise challenging to produce. We also demonstrate and monitor biotin-avidin binding on such a membrane, which will then serve as a platform for a wide range of biosensing applications. The QCM-D technique could be extended to both fundamental studies and applications of other covalent and non-covalent interactions in 2-dimensional materials.

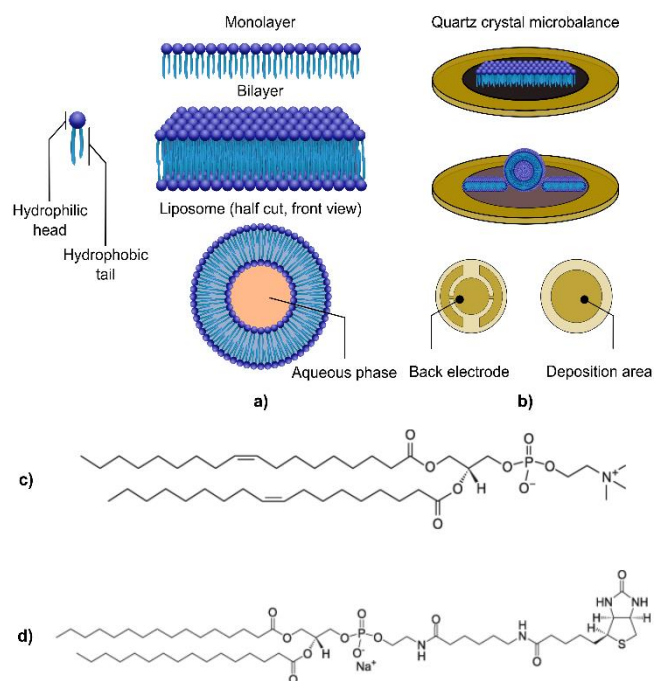
## Introduction

Graphene is a versatile 2-dimensional (2-d) nanomaterial which has attracted particular attention of scientists in the field of biological sensors [1] and biotechnology [2]. Graphene's large surface area [3], biocompatibility [4] and ease of functionalization [5], [6] provide opportunities for biomedical applications [7], [8]. Graphene derivatives can solubilize and bind drug molecules and thus have the potential to be drug delivery vehicles [9]. Such properties can be exploited to increase the sensitivity of biosensors [10] and may act as a supporting platform for the construction of biological detection arrays [11], [12]. Graphene oxide (GO) has played an important role in the development of electrochemical [10], [13] and mass-sensitive sensors [14], [15] and inclusively it has shown strong antibacterial activity [16] by affecting the integrity of the cell membrane [17], which is formed by a continuous lipid bilayer. In GO, the main surface functional groups are hydroxyls and epoxies [18], with carboxylic acids and other keto groups on the edges [19]. GO retains *sp*<sup>2</sup>-carbon domains as well as *sp*<sup>3</sup>-carbon groups, endowing it with both hydrophobic and hydrophilic domains, respectively [20]. A majority of such functional groups can be removed upon treatment with a reducing agent, such as L-ascorbic acid [21] or hydrazine [22], or thermally [23] to form reduced (r)GO, which is overall significantly more hydrophobic, comparable to pristine graphene.

Exploring different routes for the construction of supported lipid membranes (SLMs) (Scheme 1a), such as supported lipid bilayers (SLBs) or monolayers is pertinent since they are useful platforms for the study of fundamental cell functions and signaling, cell-cell

interactions, drug delivery and biosensing [24]. SLMs help to establish a model for the cell membrane and can serve as the key component of biosensor devices. The most common membrane lipids are phospholipids; amphiphilic molecules composed of hydrocarbon chain tails attached to a phosphate head group.

Here we present the study of the adsorption and rupture of small unilamellar vesicles (SUVs) (typically <100 nm) on GO- and rGO-substrates, monitored using the quartz crystal microbalance with



**Scheme 1.** Schematic representation of lipid membranes from the basic lipid unit. a) The three possible lipid structures studied b) Depiction (not drawn to scale) of a lipid monolayer on reduced graphene oxide and intact vesicles supported on graphene oxide on top of a Quartz Crystal Microbalance chip c) DOPC molecular structure d) Biotinyl cap PE molecular structure.

<sup>a</sup> School of Materials and National Graphene Institute, University of Manchester, Manchester M13 9PL UK.

<sup>b</sup> Biomolecular Analysis Core Facility, Faculty of Life Sciences, University of Manchester, M13 9PL UK.

<sup>c</sup> School of Computer Science, University of Manchester, Manchester M13 9PL UK.

<sup>†</sup> Corresponding author email: aravind@manchester.ac.uk

Electronic Supplementary Information (ESI) available: [details of any supplementary information available should be included here]. See DOI: 10.1039/x0xx00000x

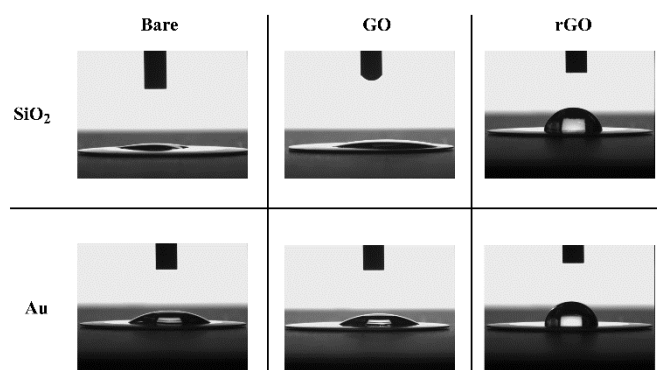


**Fig. 1** Optical images of the drop shape obtained during contact angle measurements on the bare and graphene coated SiO<sub>2</sub> and Au chip surfaces.

dissipation monitoring (QCM-D) technique [25]. Substrates used here were produced by spin coating GO on QCM-D crystals. This coating technique is a fast and reliable way that renders a uniform surface coverage with small quantities of GO dispersion (<100  $\mu\text{L}/\text{crystal}$ ) and serves as the first step to obtain an rGO film upon thermal reduction of selected substrates. Moreover, both the automation of sample injection and the real-time monitoring capabilities of the QCM-D (Q-Sense Pro, Biolin Scientific, Gothenburg, Sweden) system improve the experimental performance and simplifies the interpretation of the dynamics of membrane formation.

The interaction of graphene derivatives and phospholipid membranes using different techniques, such as AFM, ellipsometry and electrochemical cells has been previously reported [26]–[34] and the results are promising in the development of highly versatile biosensors. However, the formation of different lipid structures on commonly used substrates as well as on graphene is still not completely understood. Changing the physiochemical properties and the topology of the substrate that acts as a mediator of the interaction between the phospholipids and the surface is key in establishing possible mechanistic scenarios for the adsorption and spreading into specific structures (Scheme 1a-b). On this regard, the different chemistries present in GO and rGO provide certain hydrophilic and hydrophobic degrees and surface net charge which favor the formation of specific lipid structures. The hydrophilicity of SiO<sub>2</sub> makes it the ideal surface for SLB formation via vesicle fusion which on plain Au has been difficult to achieve using the same technique. Therefore, finding adequate modifiers to obtain different surface chemistries is crucial in the development of biocompatible platforms. Accordingly, our investigation is primarily focused on the study of biomimetic lipid membranes, namely, those that fully or partially mimic the structure of the naturally occurring containment unit of the cell as well as equivalent lipidic structures with potential biomedical applications.

The formation of lipid membranes on bare and modified SiO<sub>2</sub>, Au, mica and TiO<sub>2</sub> substrates have been previously reported and discussed in depth [35]–[38]. Promoting adsorption of SUVs onto a substrate followed by spontaneous rupture and the formation of a uniform membrane involves control over various parameters such as: vesicle size [37], electrostatic force [36], ionic properties of the buffer solution [39], [40], as well as vesicle-vesicle and vesicle-substrate interactions [41]. The latter will strongly depend on the properties of the substrate therefore varying the surface chemistry will lead to different lipidic conformations which can be monitored in real time with the help of acoustic wave sensors. Specifically, the

**Table 1** Mean values of wetting contact angles measured on the bare and graphene coated SiO<sub>2</sub> and Au chip surfaces.

	SiO <sub>2</sub>	Au
<b>Bare</b>	17.34° ± 2.79°	41.32° ± 0.83°
<b>GO</b>	32.12° ± 3.18°	38.12° ± 1.43°
<b>rGO</b>	88.44° ± 1.40°	94.74° ± 1.39°

QCM system has emerged as the primary instrument for ultra-sensitive mass detection (<1 ng/cm<sup>2</sup>) [25]. The QCM-D technique has drawn great interest as reported in studies on lipid adsorption kinetics [36], [42], measuring vitamin-protein binding events [43], [44], studying interactions in layer-by-layer graphene-lipid structures [45] and formaldehyde detection using GO as a sensing layer [46]. Modifying the supporting substrate to obtain different lipidic structures is one common approach, e.g. creating a hydrophobic layer through the deposition of -thiol self-assembled monolayers (SAMs) [41], using polymers as cushions [47] or using SAMs of organosulfates and organophosphates [48] have been reported. These modifiers are mostly used to provide specific functional groups that confer hydrophilic or hydrophobic domains, to act as spacers for further protein insertion into the membrane or to change the charge of the substrate.

Graphene's high surface area, biocompatibility, ease of functionalization and electrical properties makes it a great candidate as a surface modifier with similar simplicity of SAMs [47]. On this regard, GO is particularly interesting from its multiple functionalities. A large amount of research is devoted to understand how lipids interact with graphene to form well-defined lipidic structures and is an emerging area of investigation. Recently, Tabaei *et al.*, [49] reported the formation of a lipid monolayer on pristine graphene grown via the chemical vapor deposition (CVD) technique and then transferred to a SiO<sub>2</sub> coated QCM-D chip. Then, through the vesicle fusion technique and via a solvent-assisted lipid bilayer method the authors reported the formation of a supported layer of unruptured vesicles and a lipid bilayer on oxidized CVD graphene, respectively. Their findings are in line with previous reports which have highlighted the pivotal role that both the hydrophilic and hydrophobic interactions play in the support of lipid membranes [26], [50]–[52]. One disadvantage of the growth of graphene through the CVD technique and transfer onto a supporting substrate is that it involves a harsh atmosphere. In this regard, the annealing temperature to obtain an rGO film reported in this work is relatively low (180 °C), in contrast to the high temperatures (> 900 °C) reached for thermal reduction [20], [53]. In contrast, using graphene dispersions, like GO, for the formation of thin film coatings offers a fast route to achieve a surface with tunable hydrophobicity through thermal reduction, which in consequence helps to recover most of the properties of pristine graphene. Therefore, we propose a friendly method to obtain graphene-based acoustic wave biosensors.

In this report, we present the adsorption dynamics of zwitterionic lipid vesicles on two traditional substrates, SiO<sub>2</sub> and Au, whose hydrophobicity is modified by two graphene derivatives: GO and rGO. We additionally investigated the utility of the formed lipid membranes through a biomolecular binding event, specifically between the biotin-avidin complex which is the strongest known non-covalent biological interaction [54], [55] and is used for the development of robust and highly sensitive assays useful in protein detection [56], [57]. Non-covalent intermolecular interactions involving  $\pi$ -systems are pivotal to the stabilization of proteins, enzyme-drug complexes and functional nanomaterials [5], [58]. One

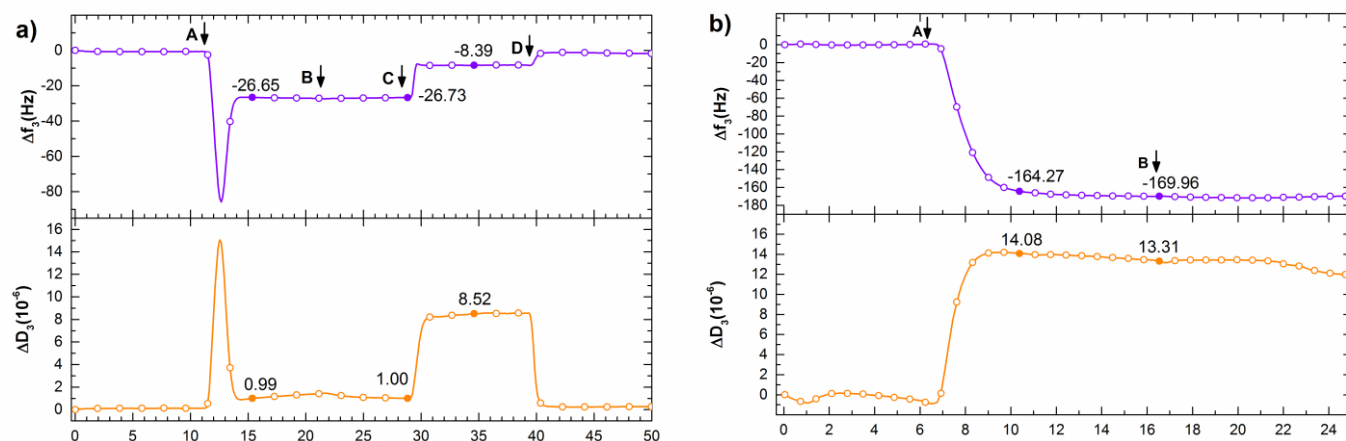


**Fig. 2** Frequency (purple, top) and dissipation (orange, bottom) response from the adsorption of DOPC on bare substrates: **a)** on bare  $\text{SiO}_2$  and **b)** bare Au. Steps: **(A)** DOPC injection, **(B)** buffer rinse, **(C)** SDS rinse, **(D)** final buffer rinse.

possible route to experimentally accomplish this binding event is by presenting the avidin protein dispersed in buffer to lipid membranes formed from biotinylated lipid vesicles that have been adsorbed, and in some cases ruptured and reorganized on a supporting substrate.

## 2. Experimental methods

### 2.1 Solutions and reagents preparation

GO dispersions were prepared by oxidizing graphite flakes according to a modified Hummers method [59] followed by exfoliation and purification, as described in the electronic supporting information (ESI).

Detailed protocol for the preparation and assembly of phospholipid membranes is presented in the ESI. Briefly, the buffer solution was prepared with 10 mM HEPES (4-(2-hydroxyethyl)-1-piperazineethanesulfonic acid) buffer from powder (Sigma Aldrich), 100 mM NaCl, and 5 mM  $\text{MgCl}_2$ , all then diluted in ultrapure water (18.5 M $\Omega$ , MilliQ). The pH was corrected to 7.4, dropwise with a solution of NaOH. This buffer solution was filtered with 0.22  $\mu\text{m}$  pore-size nylon membranes before each experiment and stored in the fridge for up to two weeks.

To prepare 1 mL of DOPC lipid vesicles 1 mL of 2.5 mg/mL DOPC (1,2-dioleoyl-sn-glycero-3-phosphocholine) lipid (Avanti Polar Lipids) dispersed in chloroform, was dried under a stream of nitrogen before resuspending in 10 mM HEPES. For the binding studies, 10 % biotinyl cap PE lipid were mixed to the final concentration of 10% total lipid in chloroform before drying. The functionalized lipid was hydrated with the HEPES buffer solution and subsequently extruded more than 23 times, as recommended by Cho's protocol [36], using 50 nm pore-size polycarbonate membranes to obtain vesicles with a diameter size distribution of  $\sim 80$ –110 nm, analyzed via dynamic light scattering (DLS, Malvern Zetasizer Nano-S) (data not shown).

Avidin from egg white (Thermo Fischer Scientific) from a stock concentration of 1mg/mL was diluted to 50  $\mu\text{g/mL}$ . Finally, the extruded lipid was aliquoted with a ratio of 1:10 (lipid:buffer) and stored in the freezer at  $-20^\circ\text{C}$  for up to two weeks to ensure vesicle stability.

### 2.2 QCM chips preparation and equipment setup

AT-cut piezoelectric quartz crystals from Q-Sense (Biolin Scientific, Gothenburg, Sweden) with a fundamental frequency of 5 MHz were used in all experiments.  $\text{SiO}_2$  and Au coated crystals

were first immersed in a 2% solution of sodium dodecyl sulfate (SDS) and sonicated in an ultrasonic bath during 25 minutes, rinsed with copious amounts of ultrapure water, then soaked in 99% ethanol for 10 min, then dried under a soft beam of nitrogen gas and immediately placed inside a UV/Ozone system to be treated for 30 min. Crystals were spin coated at 3500 rpm during 2 min (Laurell Tech., WS-650MZ) using the final dilution of GO (0.5 mg/mL).

For the thermal reduction of GO coated crystals to obtain an rGO film, GO coated sensors were placed in the oven at  $180^\circ\text{C}$  under vacuum (Towson + Mercer, EV018) during 20 hours.

The Q-Sense Omega Auto (Q-Sense, Gothenburg, Sweden) system was used to monitor the adsorption kinetics of lipid vesicles on bare and coated sensors and record the frequencies (3<sup>rd</sup> to the 7<sup>th</sup> harmonics) and dissipation values. We report the value for the 3<sup>rd</sup> overtone for both frequency ( $\Delta f_{n=3}/3$ ) and energy dissipation ( $\Delta D_{n=3}/3$ ) components. Values at other overtones can be found in the ESI.

For the wetting properties analysis, a Kruss DSA100 (Hamburg) system was used measure the wetting contact angles (WCAs) for the bare, GO- and rGO-coated QCM chips. A manually controlled syringe was used to cast sessile drops ( $\sim 5 \mu\text{L}$ ) of DI water on top of the substrates under study. An ImageJ plugin for contact angle measurement developed by Marco Brugnara [60] was used to compute the WCAs (Table 1) through a manual ellipse/circle fitting method.

## 3. Results and discussion

### 3.1 Membrane formation overview

Figure 1 shows the DI water droplets formed on the surface of the QCM crystals (see ESI for extended wetting analysis). The corresponding contact angles are summarized in Table 1. Preference for intact vesicle adsorption and/or spreading into a mono- or bilayer is influenced by the hydrophobicity or hydrophilicity of the deposition substrate. Removing organic contaminants by means of chemical agents and UV/Ozone treatment is crucial to render a substrate hydrophilic [61]. On this regard, the formation of a SLB requires a hydrophilic substrate, where a critical coverage of adsorbed vesicles must be reached first, since vesicle-substrate interactions usually do not commence individual vesicle rupture [36]. In particular,  $\text{SiO}_2$  has been the most widespread substrate for the formation of SLBs and the adsorption dynamics is well understood.

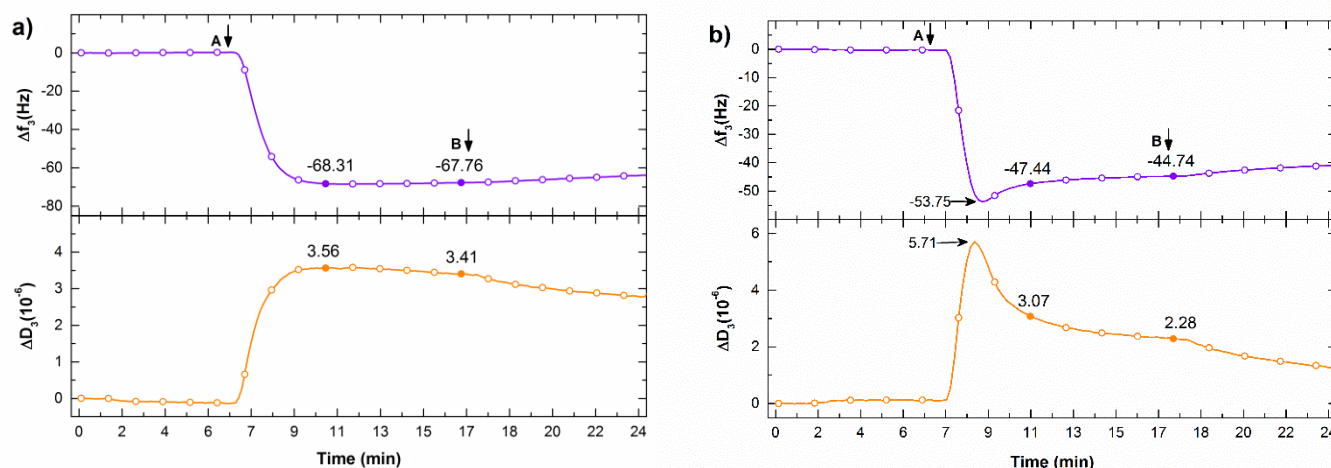


**Fig. 3** Frequency (purple, top) and dissipation (orange, bottom) response from the adsorption of DOPC on **a)** GO-coated SiO<sub>2</sub> and **b)** GO-coated Au. Steps: (A) DOPC injection and (B) buffer rinse.

On the other hand, the hydrophobic vesicle-substrate interaction has been considered as the primary driving force in the formation of a lipid monolayer [35]. With respect to gold, in an early study Smith [62] stressed the effects of carbonaceous contamination on the hydrophilicity of a clean gold substrate turning it hydrophobic. This claim is supported by Gardner and Woods [63] who demonstrated that when organic species are present, the surface of gold is hydrophobic. Therefore, we stress the importance of an adequate cleaning procedure of this sensor substrate to minimize undesirable effects of contaminants present on the working electrode of the QCM crystal. In spite of the fact that avoiding organic and inorganic contamination on the surface of gold is a challenging task, our analysis of the WCA (Table 1) shows that both the Au and SiO<sub>2</sub> QCM chips are hydrophilic as a result of our cleaning procedure, where the SiO<sub>2</sub> substrate is substantially more hydrophilic. In particular, spreading of vesicles on Au is not straightforward since it has produced conflicting results [35], [41], [64], [65]. Amongst the properties of gold, we find biocompatibility, inert nature, affinity with -thiol group and low electrostatic repulsion to zwitterionic lipids making this noble metal a good candidate for the formation of SLMs, therefore, whether clean Au promotes only vesicle adsorption or adsorption followed by spontaneous rupture was investigated here as a control and was also used as a support for the graphene coatings. Finally, the adsorption of vesicles is influenced by the presence of electrolytes and the ionic strength of the buffer solution. Both parameters have shown to affect the lipid-substrate interaction by means of the charge of the lipids head groups and the net substrate charge [39], [52]. These characteristics altogether constitute the main driving forces to promote vesicle adsorption and eventual fusion of DOPC vesicles to form a uniform membrane [52].

We have investigated the effect of GO and rGO on the assembly of different lipid membrane structures and in combination with the QCM-D technique we proposed them as suitable platforms for the detection of biomolecular interactions. All experiments were performed by following an adapted version of the protocol proposed by Cho and coworkers [36] (for detailed protocol, see ESI). Bare control QCM-D crystals were used in parallel on each of the reported measurements. Results obtained from the control chips were consistent throughout the experimental routines.

### 3.2 SLMs on bare substrates

#### 3.2.1 Formation on bare SiO<sub>2</sub>

First, we report the lipid adsorption kinetics on bare SiO<sub>2</sub>, as shown in Figure 2(a). After lipid injection (step A), a high frequency downshift indicates that vesicles are adsorbed intact on the surface reaching a critical coverage before they break and spread into a uniform membrane. Within less than 2 minutes the frequency increases stabilizing at -26.65 Hz with a dissipation of  $0.99 \times 10^{-6}$  confirming the formation of a bilayer. This energy dissipation value is somewhat higher than the typical reported values during the formation of a SLB ( $< 0.5 \times 10^{-6}$ ) [35], [42], [49], [61] denoting that our bilayer is slightly less rigid than previous reports. We emphasize that the observed fast rupture is due to the effect of the Mg<sup>2+</sup> ions on the reduction of critical coverage thus accelerating the phase of vesicle fusion [39]. The adsorbed lipid remains stable even after a buffer rinse (step B) confirming the formation of a rigid and uniform membrane. After washing out the QCM chip with SDS solution (step C), an increase in the energy dissipation to a median value of  $8.52 \times 10^{-6}$  shows that some unadsorbed lipid was removed from the surface. Finally, after rinsing with buffer (step D) the initial baseline is recovered, indicating that the crystal has been fully cleansed. The values for the frequency shift and stabilization throughout the control experiment are in line with the results reported by Keller [35] and Cho [36] on the formation of supported lipid bilayers on clean SiO<sub>2</sub> and SiO, respectively.

#### 3.2.2 Formation on bare Au

Similarly, we investigated the adsorption of DOPC vesicles on clean Au. We point at the hydrophilic-hydrophilic interaction between the lipid heads and the substrate as the main force in the formation of a vesicular layer. The lower hydrophilicity from this substrate does not favor any noticeable rupture and a monotonic vesicular adsorption is obtained. The adsorption of intact vesicles on bare Au is corroborated by the report by Liu and Chen [17] in which a supported vesicular layer was required for the evaluation of the rupture of vesicles in the presence of GO. It should be noted that in both reports we used identical Au QCM chips (Qsx-301). In addition, the ionic strength from our buffer is not enough to promote vesicle fusion and liposomes adsorbed intact without rupture. This is in contrast with previous reports that have stressed the importance of divalent ions, as Ca<sup>2+</sup>, as mediators in the formation of SLBs on gold [36], [41] i.e. by increasing the deformation of DOPC lipid vesicles [40]. Interestingly, Marques et al. [41] reported the inhibitory effect

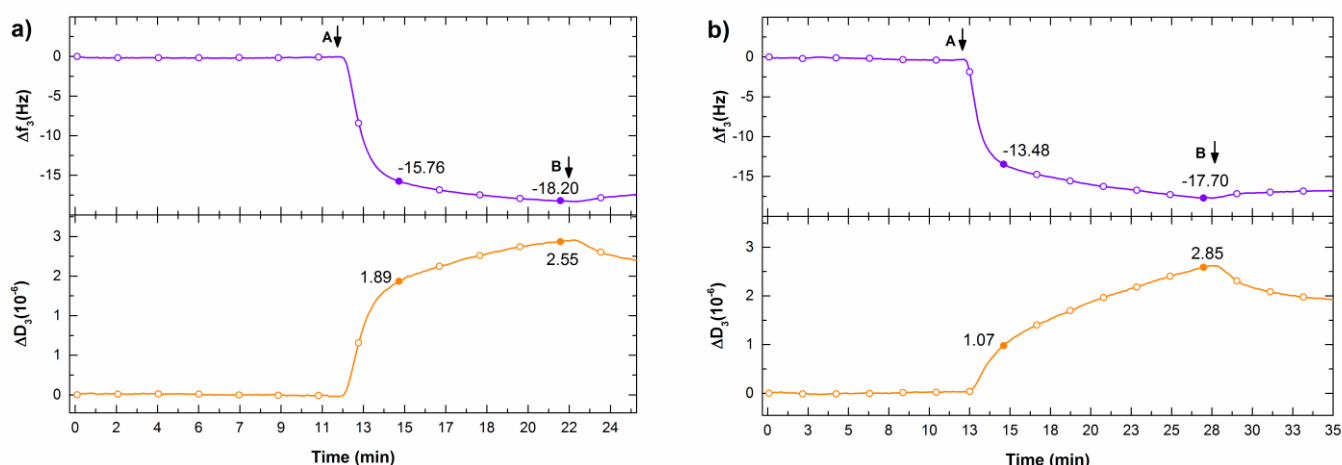


**Fig. 4** Frequency (purple, top) and dissipation (orange, bottom) response from the adsorption of DOPC on **a)** rGO-coated SiO<sub>2</sub> and **b)** rGO-coated Au. Steps: (A) DOPC injection and (B) buffer rinse.

of NaCl on the formation of lipid bilayers on gold, leading to tubular structures. We indeed tested their experimental conditions (data not shown) using a gold QCM substrate, preparing buffer solution without NaCl and keeping the Mg<sup>2+</sup> ions. However, the results did not match, perhaps because both the lipid composition (binary lipid vs single lipid) and surface topography differ between our studies. In their study, Marques and coworkers annealed the gold substrate at direct high temperature to obtain smooth micro-domains, while we used the QCM crystals as-received, namely without any other treatment than thorough cleaning, therefore keeping the inherent roughness of the substrate. It has been established that controlling the roughness of a substrate has direct impact on the structure of the membrane to be deposited [66].

The event of intact vesicle adsorption is shown in Figure 2(b) as a high frequency shift (the highest amongst all experiments) of -164.27 Hz and an energy dissipation of  $14.08 \times 10^{-6}$ , values attributable to the size of vesicles suggesting the high mass loading of the crystal with a non-homogeneous vesicular membrane that releases considerable amounts of energy during its formation and stabilization. In addition, we must consider the added mass of buffer trapped within and between the vesicles. The high dissipation value indicates that the ad layer is not rigid, rather viscoelastic. Finally, after rinsing with buffer (step B) the slight decrease of  $\Delta D_3/3$ , whilst the frequency remains constant, shows that the vesicles that conform the membrane are close packed and during this stage a lateral shift occurs, as indicated by the energy dissipation variation, with negligible loss or gain of mass. As mentioned before, we highlight the role of the roughness of the Au surface to favor the placement of intact vesicles. AFM topography of our Au QCM crystals is included in the ESI and shows a less smooth surface compared to the SiO<sub>2</sub> substrates. In a report from Li *et al.* [64] it was established that surface roughness plays a pivotal role in the formation of SLBs on a gold substrate through AFM studies on annealed gold electrodes. During a flame annealing process, clean and large gold grains with atomically flat terraces are produced which help in the promotion of vesicle fusion after lipid deposition. Such atomically smooth surfaces are not present in our crystals. Similar to our results, they indicated having obtained unfused vesicles on rough gold QCM surfaces.

As mentioned before, the electrostatic interaction plays a pivotal role on the formation of SLBs. On this regard, previous reports

denoted that negatively charged intact vesicles adsorb onto a titanium oxide or a gold substrate without spontaneous rupture to form SLBs in the absence of divalent ions, like Ca<sup>2+</sup> [36], [67]. In our study, however, a similar situation occurs with a zwitterionic (neutrally charged) single lipid on bare gold even under the effects of Mg<sup>2+</sup> ion, which has shown similar strength in the promotion of vesicle rupture [48]. In their protocol, Cho *et al.* [36] stressed the necessity for a negatively charged lipid in combination with calcium ions for the formation of SLBs on titanium oxide. As a matter of fact, they stated that their procedure is not suitable for forming single-component zwitterionic SLBs (as DOPC) on titanium oxide, which possesses similar biocompatibility and electrical properties to gold. To overcome this limitation, they proposed and tested the use of an amphipathic AH peptide as a vesicle-destabilizing agent which successfully promoted vesicle deformation and subsequent rupture into a uniform SLB. Overall, SLB formation demands specific surface properties such as surface charge density and hydrophilicity. Therefore, the use of specific agents, including surface modifiers, is a common way to help the promotion of vesicle rupture and GO naturally emerges as a good candidate due to its richness in functional groups that confer this material its distinctive properties. Accordingly, we discuss next the interaction between GO-coated substrates and lipid vesicles.

### 3.3 SLMs on GO-coated substrates

According to the widely accepted Lefr-Klinowski model [20], GO sheets have a high number of oxygen groups that confer the material interesting physicochemical properties. Particularly, on the basal plane hydroxyl (-OHs) and epoxy groups give GO its hydrophilic nature [20]. In addition, ionized carboxyl groups (-COOH) at the edges make GO sheets negatively charged [68]. We confirm the presence of these groups in our GO through XPS (see ESI). Previous studies have reported that lipid head groups control the interaction between charged lipids and GO, showing that these have a strong electrostatic interaction with the negatively charged carboxyl groups of GO [28], [69]. Some studies consider that even van der Waals forces might participate on the association between GO and lipids [68]. Specifically, neutrally charged liposomes (as DOPC) associate with the oxidized hydrophilic regions of GO sheets. In addition, system hydration is believed to importantly contribute to the

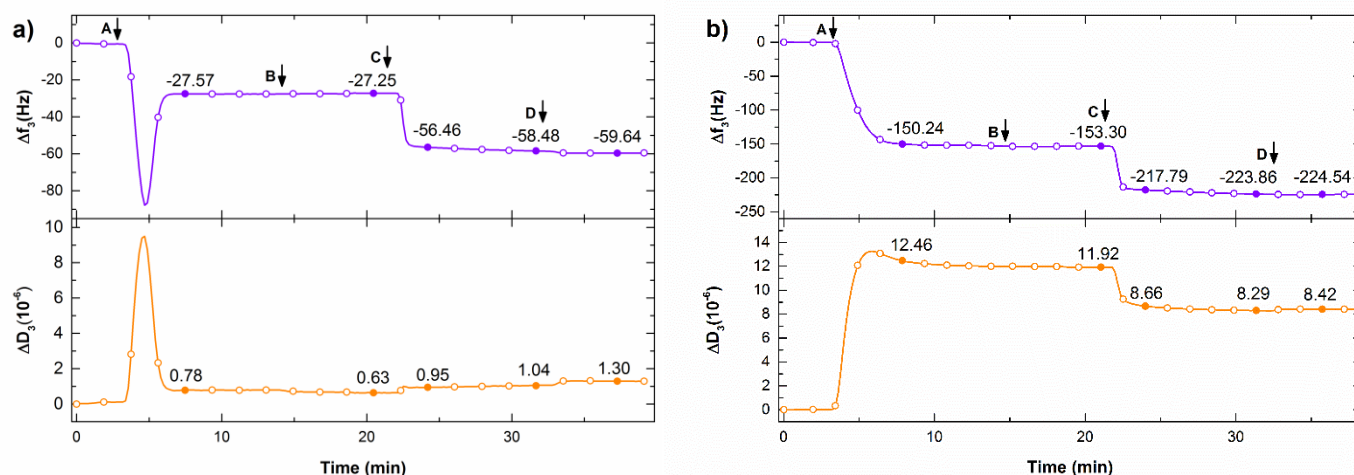


**Fig. 5** Frequency (purple, top) and dissipation (orange, bottom) response from the biotin-avidin binding event **a)** on a lipid bilayer supported on bare  $\text{SiO}_2$  and **b)** on a vesicular lipid membrane supported on bare Au. Steps: **(A)** DOPC with biotin caps injection, **(B)** buffer rinse, **(C)** avidin injection, **(D)** final buffer rinse.

interaction, since water molecules mediate the hydrogen bonding between the carboxyl and the phosphate oxygen present in the lipid headgroup [69]. In a recent work, Willems *et al.* [70] have shown, via coarse-grained molecular dynamics simulations, that preformed lipid bilayers and inverted lipid monolayers supported on GO sheets when immersed in water rapidly reorganize into bicelle-like structures. Such rearrangement is thought to be driven by lipid headgroup interactions and was explained by the polarity from the oxygen-containing functional groups in GO. This finding highlights the effect of hydration of the system, thus supporting the vastly accepted hypothesis of the hydrogen bonding between the carboxyl groups of GO and the phosphate head group from DOPC [71]. Willems' and coworkers work preceded a similar study by Rivel *et al.* [72] that stressed the competition between the amphiphilic nature of the phospholipid, the hydrophobicity of graphene (also present as hydrophobic domains on GO sheets) and the hydrophilicity of water during the formation of single and multilayer of lipids on graphene.

### 3.3.1 Formation on GO- $\text{SiO}_2$

The formation of lipid membranes supported on GO-coated  $\text{SiO}_2$  quartz crystals is shown in Figure 3(a). The frequency shift ( $\Delta f_3/3$ ) reaches an initial stabilization value of -68.31 Hz after vesicle injection (step A). Similar to the previous result, we assume the considerable mass uptake due to buffer trapped within the aqueous phase of liposomes and the mass of buffer between them. The energy dissipation value of  $3.56 \times 10^{-6}$  indicates the formation of a soft membrane conformed by lipid vesicles which are strongly adhered to the edges of the GO flakes and sparsely distributed on their surface, as it has been previously proposed [69], [73]. From the frequency dissipation response, vesicles adhere without noticeable rupture, as a possible effect of bare  $\text{SiO}_2$  regions during the coating procedure thus indicating a good coverage of the substrate. In this regard, Furukawa *et al.* [74] reported that GO blocks the formation of SLBs on a  $\text{SiO}_2$  substrate where GO flakes are present. This effect is explained by the amphiphilic nature of this graphene derivative due to the presence of both  $\text{sp}^2$  and  $\text{sp}^3$  domains. Additionally, it was established by Frost *et al.* [45], [75] that liposomes do not rupture when adsorbing to GO. They found that rupture of vesicles is affected by both the dimension of the GO flakes and the diameter of the liposomes. They observed that liposomes fully rupture upon further

addition of GO flakes, after they have adsorbed to large GO sheets (0.5–5  $\mu\text{m}$ ) obtaining multilayered structures of lipid membranes and GO. Interestingly, their hypothesis is that for vesicle rupture to occur, lipid vesicles must be exposed to two GO sheets, one on each side, where GO sheets are of the same size or larger than the cross-sectional area of the liposome. On this regard, it is evident that in our investigation we exposed only one side of the liposomes to GO flakes when they were adsorbed to the GO-coated substrate hence no rupture would be expected. Our result is in good agreement with a previous report on the adsorption of intact vesicles without fusion on oxidized CVD graphene transferred to a  $\text{SiO}_2$  substrate [49], however the adsorbed mass in our experiment was higher perhaps due to the higher hydrophilicity of our GO coated crystals, promoting then a higher attraction vesicles. Interestingly, our results are in opposing direction to the findings of Okamoto *et al.* [73] who reported the formation of single and double bilayers via vesicle fusion on GO flakes supported on  $\text{SiO}_2$  in the presence of divalent ions, like calcium. We point out at the topographic differences between the substrates used in our studies and their effect on the adsorption and fusion of lipid vesicles. In their study, SLBs were formed by incubation of DOPC vesicles on a GO/ $\text{SiO}_2$ /Si substrate and analyzed using AFM. During the substrate preparation stage, large blank  $\text{SiO}_2$  regions were still present after the deposition of GO solution, while in our study we aimed to obtain a uniform coverage of the substrate. Based on their results, the formation of bilayers and double bilayers on GO sheets is explained as an effect of its surface heterogeneity, however their findings are not conclusive on this matter. As we discussed before,  $\text{SiO}_2$  is well known to promote SLB formation due to its hydrophilic property, therefore the strong effect that  $\text{SiO}_2$  has on the fusion of DOPC vesicles might be the leading interaction in that scenario. We reason that after the vesicle rupture events originated at the blank  $\text{SiO}_2$  regions, fragmented lipid is rapidly attracted by and mobilized onto the regions covered with GO. This hypothesis is supported by previous reports by Hirtz *et al.* who have shown the self-limiting spreading of DOPC on graphene [34], [76] and, as previously discussed, lipids rapidly reorganize into different lipidic structures in aqueous media [70], [72]. The contrasting homogenous hydrophilicity of  $\text{SiO}_2$  and the distributed hydrophobicity from the  $\text{sp}^2$  domains from GO sheets might lead such interaction. On this regard, the QCM-D technique excels the

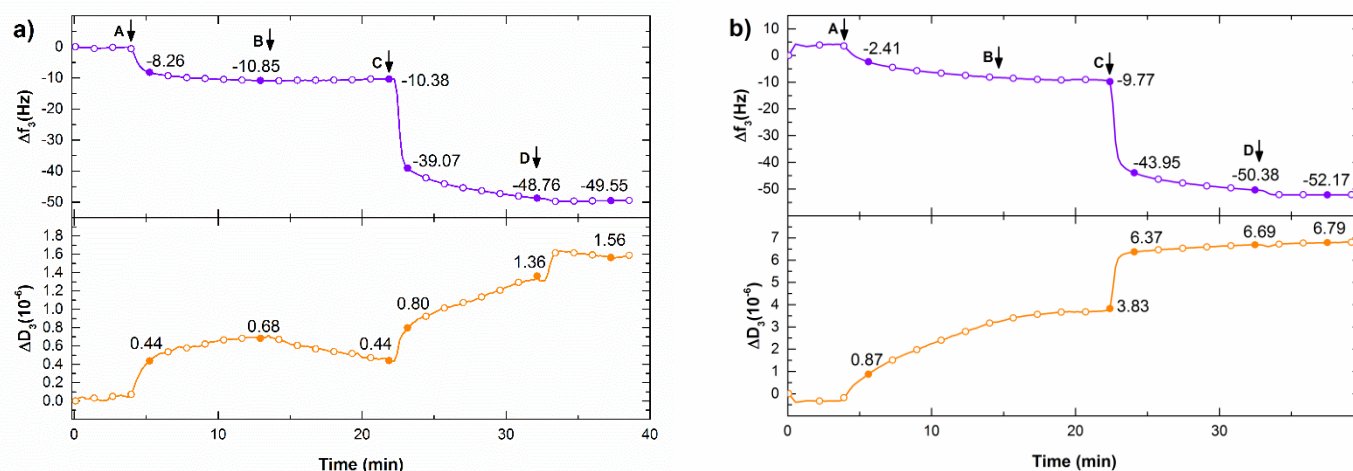


**Fig. 6** Frequency (purple, top) and dissipation (orange, bottom) response from biotin-avidin binding event on a lipid monolayer supported **a)** on rGO-coated SiO<sub>2</sub> and **b)** on rGO-coated Au. Steps: (A) DOPC with biotin caps injection, (B) buffer rinse, (C) avidin injection, (D) final buffer rinse.

AFM topographical analysis on the capability to monitor both dynamically and in real-time the adsorption of lipids on specific substrates. It is important to highlight the relevance of vesicular lipid membranes for certain applications, e.g. where lipid vesicles are used as drug carriers and the release of drugs trapped in the aqueous phase must be time controlled through the addition of vesicle destabilizers that promote rupture.

### 3.3.2 Formation on GO-Au

On the other hand, on the GO-coated gold chip (Figure 3(b)), vesicles are adsorbed intact after lipid injection (step A). The frequency shift reaches a critical coverage point at a value of -53.75 Hz (arrow) indicating the formation of a membrane of intact vesicles which in less than one minute is followed by partial vesicle rupture, shown as a subsequent frequency increase and stabilization to a value of -44.74 Hz before the buffer rinse step (B). After reaching the critical coverage point, the energy dissipation exponentially decreases from a maximum of  $5.71 \times 10^{-6}$  to a value of  $2.28 \times 10^{-6}$ , before rinse. These factors indicate a considerable release of energy during the initial stabilization stage, where vesicles stack then squash and the weakly adsorbed lipid distributed on the surface detaches after buffer rinse (step B), suggesting the gradual compaction of the membrane and a spatial redistribution of the initial vesicular membrane into a different lipidic structure. In contrast to the previous result on GO-coated SiO<sub>2</sub> chip, the lower value of adsorbed mass on the GO-coated Au chip after stabilization indicates that after leaking buffer from within the aqueous phase, some ruptured vesicles reorganize to more likely form bicelle-like structures, as previously discussed from the results on GO in water by Willems and coworkers. Therefore, our results point toward a mixed membrane conformed of intact vesicles and bicelle-like islands.

In both cases, lipid vesicles interact with a heterogeneous surface chemistry present on the GO sheets on these GO-coated chips. We reason that the presence of both hydrophilic/hydrophobic domains establishes an equilibrium on the vesicle-substrate interaction forces which might be altered by the differences on the intrinsic topography of the substrates. Based on our WCAs (Table 1), the GO coating on the smoother SiO<sub>2</sub> substrate is not hydrophilic enough to promote rupture like its bare counterpart while GO on gold, showing slightly more hydrophilic regions than bare gold, leads the adsorption of

vesicles followed by partial rupture, as shown in Figure 3(b). In addition, following the previously discussed hypothesis posed by Frost and coworkers, such rupture might occur at specific sites where some vesicles are partially wrapped by GO flakes present on some valleys of the rough gold substrate.

In addition to the hydrophilic vesicle-substrate interaction, we point at the electrostatic force between the negatively charged GO regions and the dipole headgroup of the zwitterionic lipid as the main driving forces for the adsorption of intact vesicles. From our results, it is evident that the ionic strength of the buffer and the cation bonding with the phosphate group of DOPC only promotes partial vesicle rupture upon completion of the critical coverage which in the case of the GO-SiO<sub>2</sub> (Figure 4(a)) the mass loss after rupture is negligible in comparison to the desorbed lipid on the GO-Au chip after partial rupture and stabilization.

### 3.4 SLMs on rGO-coated substrates

Removing the oxygen groups by the thermal reduction of GO coated substrates effectively changes the surface chemistry leading to a highly hydrophobic surface, as seen on the substantial increase on the contact angle after the thermal treatment of the QCM-D sensor set (Table 1). Thus, a new group of measurements were carried out to study the adsorption dynamics of DOPC vesicles on rGO substrates.

#### 3.4.1 Formation on rGO-SiO<sub>2</sub>

Figure 4(a) shows the monotonic response for the formation of a lipid monolayer on rGO-coated SiO<sub>2</sub> chip. After injecting the lipid vesicles (step A), vesicle rupture and spreading into a monolayer occurs. This distinctive adsorption and instantaneous rupture is due to the interaction between the hydrophobic regions of rGO [77] and the hydrophobic fatty acid chains from lipid tails. It has been reported that in the formation of this type of membrane via vesicle fusion on hydrophobic substrates such as a methyl-terminated SAM [35] and CVD graphene [49] a frequency shift of around -13 Hz is expected. In our case  $\Delta f_3/3$  varies from an initial stabilization value of -15.76 Hz to a final frequency of -18.20 Hz with a dissipation of  $2.55 \times 10^{-6}$  before buffer rinse (step B). These values somewhat differ from previous reports on the formation of uniform lipid

monolayers, however they point toward the formation on a non-homogeneous monolayer. On this regard, we hypothesize that individual lipid molecules are attracted during vesicle rupture to the reduced GO sheets with higher hydrophobicity, forming small islands that support an additional lipid membrane on top on them, as it was pictured by Tsuzuki et.al. [27]. Furthermore, the higher mass uptake can be attributed to a wetting film present in the interface. Interfacial water layers have been observed under graphene membranes adhered to sapphire substrate, uniformly trapping water that lifted the edges of graphene sheets, in consequence adding more mass to the sensor [78]. We draw attention to the structural and chemical differences between a transferred CVD graphene sheet and a thermally reduced GO coating. While the first can be considered as a highly crystalline film that might be mono- or few-layer graphene, the second cannot be regarded as a single continuous film, rather a group of overlapping sheets randomly arranged on the surface creating multilayer graphene-like platelets that may preserve different functionalities due to an imperfect thermal reduction process.

### 3.4.2 Formation on rGO-Au

Similarly, on an rGO-coated Au chip (Figure 4(b)), after lipid injection (step A) instantaneous rupture of vesicles occurs with an initial  $\Delta f_3/3$  value of -13.48 Hz reaching a final frequency shift of -17.70 Hz indicating the formation of a lipid monolayer membrane. The final dissipation value of  $2.85 \times 10^{-6}$  shows that the membrane has viscoelastic properties.

Considering the variations between the initial and final values obtained for the frequency shift in both samples, rGO-SiO<sub>2</sub> and rGO-Au, our results are within range of previous reports on the formation of lipid monolayers on hydrophobic graphene [49].

## 3.5 Graphene-SLMs as biomolecular interactions platforms

Finally, we examined the biomolecular interaction between the Biotin-Avidin complex supported by lipid membranes formed on bare and rGO-coated substrates. The biomolecular interaction associated with a vesicular layer, as those from the GO-coated substrates, is out of the scope of this study and has no biotechnical relevance from the perspective of biomimetic membranes.

Our aim was to investigate the kinetics of the lipid adsorption and binding event on the SLMs, especially on graphene due to the similarities between rGO and pristine graphene. On this regard, Hirtz *et al.* [79] have reported the assembly of inverted phospholipid bilayers (where the hydrophobic tails are facing towards the water/air media and the supporting layer holds the hydrophilic heads) on exfoliated graphene in air, via the dip-pen nanolithography technique. Interestingly, after immersion in buffer of the lipid bilayer they observed a rearrangement into a monolayer with the hydrophilic headgroups facing outwards, more likely happening due to a strong interaction between the hydrophobic surface of rGO and the lipid tails. Obtaining right oriented lipid monolayers is crucial in biomolecular studies in liquid media such as the insertion of peripheral proteins or the present biotin-avidin binding measurement since the interaction can only occur with the biotin molecules attached to the lipid heads.

We have obtained the experimental conditions for real-time monitoring of the detection of biomolecular interactions that can take place in biomimetic membranes supported on graphene through the vesicle fusion technique for the formation of SLMs and employing the QCM-D system. These experiments were performed by following the same process described before and the only

difference is the use of 10% biotinylated DOPC lipid vesicles for the formation of the lipid membranes. In addition, we included two extra steps: the injection of avidin protein dispersed in HEPES followed by a final rinse with clean buffer for the elimination of any residual lipid or untied protein.

### 3.5.1 Avidin-biotin binding on bare SiO<sub>2</sub> SLM

The first binding event was carried out on a lipid bilayer formed on bare SiO<sub>2</sub>, shown in Figure 5(a). Initially, the formation of a homogeneous lipid bilayer follows the same adsorption kinetics as described before. After lipid injection (step A) followed by buffer rinse (step B), both values for the frequency and dissipation of -27.25 Hz and  $0.63 \times 10^{-6}$ , respectively, validate the formation of the bilayer. At step C, avidin injection is followed by an instantaneous binding to the biotin caps attached to the lipid heads. A clean and monotonic mass uptake after protein injection occurs, with a frequency of -56.46 Hz. In addition, a low energy dissipation of  $0.95 \times 10^{-6}$  during binding (steps C-D) indicates that the attachment of avidin molecules happens without altering the structure of the previously formed rigid bilayer. Here the difference between the stable frequency value before protein injection and the final frequency at the binding event completion (step D) is  $\approx 29$  Hz for the bilayer support.

### 3.5.2 Avidin-biotin binding on bare Au SLM

In contrast, the binding event supported on a bare Au chip (Figure 5(b)) shows a frequency a value of -153.30 Hz at the end of the stabilization region (steps B-C) after the adsorption of intact vesicles (step A). Then, the frequency reaches a value of -217.79 Hz after avidin injection (step C) with a final frequency value of -223.86 Hz before rinse. This variation corresponds to  $\approx 70$  Hz. We validate this high value from the surface area of the vesicular membrane, where a myriad of biotin molecules is present at the outer layer of each liposome for the protein to bind. The overtones considerably diverged (see ESI) throughout the experiment indicating that there is frequency dependence during the shear mode of the crystal. A high dissipation value of  $12.46 \times 10^{-6}$  is reached after a slight peak during the formation of the supported lipid vesicles while  $\Delta f_3/3$  varies monotonically. This behavior is indicative of vesicle-vesicle compaction prior to the formation of a non-homogeneous soft membrane. In contrast to the vesicular lipid membrane formed on bare Au (Figure 2(b)) the frequency shift during stabilization is lower and no partial rupture occurs, perhaps due to the hydrophobic nature of biotin [55] present in the lipid heads, changing the vesicle-substrate interaction by the reduction of the hydrophilic attracting force, and thus reducing the number of adsorbed vesicles. Finally, after rinse (step D), the slight increase in both  $\Delta f_3/3$  and  $\Delta D_3/3$  to values of -224.54 Hz and  $8.42 \times 10^{-6}$ , respectively, indicates that some remaining unattached protein is dragged from saturated sites to available biotin sites to attach, similar to the previous result.

### 3.5.3 Avidin-biotin binding on rGO-SiO<sub>2</sub> SLM

Next, the lipid monolayer formed on rGO-SiO<sub>2</sub> was used as a supporting platform for the protein binding (Figure 6(a)). The frequency dissipation before avidin injection (step A) stabilized at -10.38 Hz. We consider this value within the lower limit for the formation of a lipid monolayer on graphene, according to previous reports [49]. The low energy dissipation value of  $0.44 \times 10^{-6}$  with a momentary increase to  $0.68 \times 10^{-6}$  during the monolayer formation (steps A-C), indicates that the membrane is being compacted to be

**Table 2** Summary of results

Crystal	Coating	$\Delta f_3/3$ [Hz]	$\Delta D_3/3$ [ $\times 10^{-6}$ ]	Stabilisation time	Structure type
SiO <sub>2</sub>	Bare	-26.73	1.00	10:15	Lipid bilayer
	GO	-67.76	3.41	10:00	Intact vesicles layer
	rGO	-18.20	2.55	9:53	Monolayer
Au	Bare	-169.96	13.31	10:12	Intact vesicles layer
	GO	-53.75 $\rightarrow$ -44.74	5.71 $\rightarrow$ 2.28	10:24	Intact vesicles + Bicelle-like structures
	rGO	-17.70	2.85	14:58	Monolayer

finally closely attached to the surface. The noticeable unsteady value of  $\Delta D_3/3$  throughout the lifetime of the experiment ( $\sim 38$  min) suggests that the membrane is settling onto the surface. However, the uniformity of  $\Delta f_3/3$  throughout the stabilization period (steps B–C) indicates that the membrane is rigid and the movement is parallel to the shear force of the QCM-D sensor. After injection of avidin (step C) the instantaneous frequency shift indicates a successful binding event reaching an initial value of  $-39.07$  Hz then stabilizing at  $-49.55$  Hz after buffer rinse (step D). These values represent a variation of  $\approx 40$  Hz.

### 3.5.4 Avidin-biotin binding on rGO-Au SLM

Finally, Figure 6(b) shows the adsorption kinetics of the binding event on a lipid monolayer supported on a rGO-Au chip. At the end of the membrane formation stage (steps A–C) the frequency stabilizes to a value of  $-9.77$  Hz which is close to the lower limit of the formation of a monolayer. We reason that this low value of  $\Delta f_3/3$  indicates an incomplete coverage of the substrate and the formation of rGO patches supporting islands of lipid monolayer. In this case, the frequency variation is of  $\approx 42$  Hz, which is slightly higher than the values obtained for bilayer and monolayer on SiO<sub>2</sub>. This difference can be explained from a structural point of view of the distribution of the monolayer patches on the substrate. We consider that they are spatially separated by the topography of the Au substrate, leaving exposed biotin caps attached to the lipid heads that are located at the margins of the lipid membrane, therefore increasing the available binding sites, whereas for the monolayer and bilayer on SiO<sub>2</sub> the avidin binds to the biotin present in the superficial layer of the continuous membranes. In addition, the increase in the dissipation after the binding event (step C) and buffer rinse (step D) to a final value of  $6.79 \times 10^{-6}$  shows that the membrane is not homogeneous. This behavior might corroborate our hypothesis for the structural distribution of lipid patches since the buffer flow hits them generating lateral movement, therefore increasing the energy dissipation.

## Conclusions

We have described the construction and characterization of graphene supported biomimetic lipid membranes and the biomolecular interactions that can take place on different substrates. We elucidated that both the chemical heterogeneity of GO and the nature of supporting substrate lead to different lipid structures obtaining either a membrane of intact vesicles or a mixed layer composed of intact vesicles and ruptured vesicles that reorganised into structures that resemble lipidic bicelles. In contrast, lipid monolayers were successfully obtained on both substrates coated with reduced GO, where the hydrophobicity of the supporting material reached its

highest point. In general, the formation of the range of lipidic structures presented on this work occurred in less than 15 minutes in terms of the time to become stable or for the time the response showed a monotonic behaviour.

From a general standpoint, the variability of the responses obtained for the interaction between lipids and coated substrates in the four cases under study that involved graphene is appreciable as presented in Table 2, i.e., GO-SiO<sub>2</sub>, GO-Au, rGO-SiO<sub>2</sub> and rGO-Au. This contrast of responses is explained not only from the perspective of the lipid-graphene interface but also from the effect that the underlying layer has on the graphene support. The wetting transparency effect [80] has been demonstrated in terms of the permeability of the graphene film to the hydrophilicity/hydrophobicity of the support substrate and the role that the interfacial water layer plays, transferring these forces from the substrate to the graphene surface [78]. This fact may explain with enough consistency the differences on the formation of SLMs using the same support substrate and attributable to the difference in surface chemistries.

Graphene stands as an effective route for the chemical modification of the selected substrates and as the underlying platform for the development of a mass sensitive biosensor. The interaction between lipids and graphene is strongly led by electrostatic and hydrophobic interactions between them, therefore is necessary to investigate the crucial experimental parameters to obtain reproducible and defect free membranes. The techniques for the formation of lipid monolayers have evolved, moving from the Langmuir-Blodgett technique [81] towards the vesicle fusion [35], [50] on substrates with inherent or modified hydrophobicity. Performing the latter on graphene sheets is a straightforward option for the site-selective formation of lipid monolayers due to the strong interaction between the lipid tails and the graphene plane.

Overall, our results shed light on the interaction between zwitterionic lipids and the dynamics of the physisorption to graphene platforms for potential biotechnical applications. Despite lipid monolayers do not resemble the complexity of biological membranes due to their structural simplicity, they have shown great utility on the evaluation of the interfacial organization of lipid membrane constituents and the changes in the interfacial organization upon the insertion of amphipathic compounds [82] and due to their homogeneity, stability and planar geometry lipid monolayers have been proposed over bilayers as suitable models to characterize protein-membrane interactions [83].

Following the monolayer technique, lipid monolayers have been used for the incorporation of amino acids, like antimicrobial peptides, or proteins, like cardiotoxins as their site of actuation is at the cell membrane level, binding and

disrupting the outer membrane [83]. This specific affinity to monolayers could potentially increase the sensitivity of the binding detection in comparison to a bilayer membrane.

Is of our interest to use the proposed rGO-QCM-D platforms as a biomimetic device to study the insertion and binding mechanism of tail-anchored proteins and Odorant-Binding Proteins (OBPs), a soluble protein secreted in the nasal mucus of animal species and in the sensillar lymph of chemosensory sensilla of insects. Our results will serve as the basis to achieve such biosensing system. In the future, our work will be undertaken to study the viscoelastic properties of the adsorbed membranes and binding events using models such as the Sauerbrey equation and the Voigt model to characterize the thickness and mass of the ad layers.

## Acknowledgements

DM acknowledges The National Council for Science and Technology (CONACyT), Mexico for the financial support. AV, AFV and SG acknowledge funding from the Engineering and Physical Sciences Research Council (EPSRC) grants EP/K016946/1 and EP/G03737X/1. The authors acknowledge E. W. Hill and B. Grieve for helpful discussions.

## Notes and references

- [1] X. Gan and H. Zhao, "A Review: Nanomaterials Applied in Graphene-Based Electrochemical Biosensors," *Sensors Mater.*, vol. 27, no. 2, pp. 191–215, 2015.
- [2] J. Wang, *Analytical electrochemistry*. John Wiley & Sons, 2006.
- [3] A. Geim and K. Novoselov, "The rise of graphene," *Nat. Mater.*, 2007.
- [4] A. M. Pinto, I. C. Gonçalves, and F. D. Magalhães, "Graphene-based materials biocompatibility: A review," *Colloids Surfaces B Biointerfaces*, vol. 111, pp. 188–202, 2013.
- [5] V. Georgakilas, M. Otyepka, A. B. Bourlinos, V. Chandra, N. Kim, K. C. Kemp, P. Hobza, R. Zboril, and K. S. Kim, "Functionalization of Graphene : Covalent and Non-Covalent Approaches , Derivatives and Applications," 2012.
- [6] K. Yang, L. Feng, H. Hong, W. Cai, and Z. Liu, "Preparation and functionalization of graphene nanocomposites for biomedical applications.," *Nat. Protoc.*, vol. 8, no. 12, pp. 2392–403, 2013.
- [7] H. Shen, L. Zhang, M. Liu, and Z. Zhang, "Biomedical applications of graphene," *Theranostics*, vol. 2, no. 3, pp. 283–294, 2012.
- [8] C. Chung, Y. K. Kim, D. Shin, S. R. Ryoo, B. H. Hong, and D. H. Min, "Biomedical applications of graphene and graphene oxide," *Acc. Chem. Res.*, vol. 46, no. 10, pp. 2211–2224, 2013.
- [9] K. S. Novoselov, V. I. Fal, L. Colombo, P. R. Gellert, M. G. Schwab, K. Kim, and others, "A roadmap for graphene," *Nature*, vol. 490, no. 7419, pp. 192–200, 2012.
- [10] B. Unnikrishnan, S. Palanisamy, and S.-M. Chen, "A simple electrochemical approach to fabricate a glucose biosensor based on graphene-glucose oxidase biocomposite," *Biosens. Bioelectron.*, vol. 39, no. 1, pp. 70–75, 2013.
- [11] P. Labroo and Y. Cui, "Graphene nano-ink biosensor arrays on a microfluidic paper for multiplexed detection of metabolites," *Anal. Chim. Acta*, vol. 813, pp. 90–96, 2014.
- [12] J. Choi, C. Lim, Y. Jung, D. Heon Shin, S. Bae, S. Kyung Kim, and C. Kim, "A Microfluidic-Channel Regulated, Electrolyte-Gated Graphene FET Biosensor Array for Repeatable and Recalibrated Detection of Thrombin," *Biophys. J.*, vol. 110, no. 3 Supplement 1, p. 334a, 2016.
- [13] J. Li, D. Kuang, Y. Feng, F. Zhang, Z. Xu, and M. Liu, "A graphene oxide-based electrochemical sensor for sensitive determination of 4-nitrophenol," *J. Hazard. Mater.*, vol. 201, pp. 250–259, 2012.
- [14] B. Cai, K. Hu, C. Li, J. Jin, and Y. Hu, "Bovine serum albumin bioconjugated graphene oxide: Red blood cell adhesion and hemolysis studied by QCM-D," *Appl. Surf. Sci.*, vol. 356, pp. 844–851, 2015.
- [15] Z. Yuan, H. Tai, Z. Ye, C. Liu, G. Xie, X. Du, and Y. Jiang, "Novel highly sensitive QCM humidity sensor with low hysteresis based on graphene oxide (GO)/poly (ethyleneimine) layered film," *Sensors Actuators B Chem.*, vol. 234, pp. 145–154, 2016.
- [16] Y. Tu, M. Lv, P. Xiu, T. Huynh, M. Zhang, M. Castelli, Z. Liu, Q. Huang, C. Fan, H. Fang, and R. Zhou, "Destructive extraction of phospholipids from Escherichia coli membranes by graphene nanosheets," *Nat Nano*, vol. 8, no. 8, pp. 594–601, 2013.
- [17] X. Liu and K. L. Chen, "Interactions of graphene oxide with model cell membranes: Probing nanoparticle attachment and lipid bilayer disruption," *Langmuir*, vol. 31, no. 44, pp. 12076–12086, 2015.
- [18] K. Erickson, R. Erni, Z. Lee, N. Alem, W. Gannett, and A. Zettl, "Determination of the local chemical structure of graphene oxide and reduced graphene oxide," *Adv. Mater.*, vol. 22, no. 40, pp. 4467–4472, 2010.
- [19] J. P. Rourke, P. A. Pandey, J. J. Moore, M. Bates, I. A. Kinloch, R. J. Young, and N. R. Wilson, "The real graphene oxide revealed: Stripping the oxidative debris from the graphene-like sheets," *Angew. Chemie - Int. Ed.*, vol. 50, no. 14, pp. 3173–3177, 2011.
- [20] D. R. Dreyer, S. Park, C. W. Bielawski, and R. S. Ruoff, "The chemistry of graphene oxide," *Chem. Soc. Rev.*, vol. 39, no. 1, pp. 228–240, 2010.
- [21] J. Zhang, H. Yang, G. Shen, P. Cheng, J. Zhang, and S. Guo, "Reduction of graphene oxide via L-ascorbic acid.," *Chem. Commun.*, vol. 46, no. 7, pp. 1112–4, 2010.
- [22] S. Stankovich, D. A. Dikin, R. D. Piner, K. A. Kohlhaas, A. Kleinhammes, Y. Jia, Y. Wu, S. T. Nguyen, and R. S. Ruoff, "Synthesis of graphene-based nanosheets via chemical reduction of exfoliated graphite oxide," *Carbon N. Y.*, vol. 45, no. 7, pp. 1558–1565, 2007.
- [23] S. Pei and H. M. Cheng, "The reduction of graphene oxide," *Carbon N. Y.*, vol. 50, no. 9, pp. 3210–3228, 2012.
- [24] S. G. Boxer, "Molecular transport and organization in supported lipid membranes," *Curr. Opin. Chem. Biol.*, vol. 4, no. 6, pp. 704–709, 2000.
- [25] M. Rodahl, F. Höök, A. Krozer, P. Brzezinski, B. Kasemo, F.

- H??k, A. Krozer, P. Brzezinski, and B. Kasemo, "Quartz crystal microbalance setup for frequency and Q-factor measurements in gaseous and liquid environments," *Rev. Sci. Instrum.*, vol. 66, no. 7, pp. 3924–3930, 1995.
- [26] X. Hu, H. Lei, X. Zhang, and Y. Zhang, "Strong hydrophobic interaction between graphene oxide and supported lipid bilayers revealed by AFM," *Microsc. Res. Tech.*, vol. 79, no. 8, pp. 721–726, 2016.
- [27] K. Tsuzuki, Y. Okamoto, S. Iwasa, R. Ishikawa, a Sandhu, and R. Tero, "Reduced Graphene Oxide as the Support for Lipid Bilayer Membrane," *J. Phys. Conf. Ser.*, vol. 352, p. 12016, 2012.
- [28] S. Li, A. J. Stein, A. Kruger, and R. M. Leblanc, "Head groups of lipids govern the interaction and orientation between graphene oxide and lipids," *J. Phys. Chem. C*, vol. 117, no. 31, pp. 16150–16158, 2013.
- [29] L. Wu, L. Zeng, and X. Jiang, "Revealing the nature of interaction between graphene oxide and lipid membrane by surface-enhanced infrared absorption spectroscopy," *J. Am. Chem. Soc.*, vol. 137, no. 32, pp. 10052–10055, 2015.
- [30] L. Rui, J. Liu, J. Li, Y. Weng, Y. Dou, B. Yuan, K. Yang, and Y. Ma, "Reduced graphene oxide directed self-assembly of phospholipid monolayers in liquid and gel phases," *Biochim. Biophys. Acta - Biomembr.*, vol. 1848, no. 5, pp. 1203–1211, 2015.
- [31] S.-J. Liu, Q. Wen, L.-J. Tang, and J.-H. Jiang, "Phospholipid-graphene nanoassembly as a fluorescence biosensor for sensitive detection of phospholipase D activity," *Anal. Chem.*, vol. 84, no. 14, pp. 5944–5950, 2012.
- [32] M. A. Ali, K. Kamil Reza, S. Srivastava, V. V. Agrawal, R. John, and B. D. Malhotra, "Lipid-lipid interactions in aminated reduced graphene oxide interface for biosensing application," *Langmuir*, vol. 30, no. 14, pp. 4192–4201, 2014.
- [33] M. Pittori, M. G. Santonicola, L. Ortolani, D. Gentili, V. Morandi, and R. Rizzoli, "Graphene-lipids interaction: Towards the fabrication of a novel sensor for biomedical uses," *IEEE-NANO 2015 - 15th Int. Conf. Nanotechnol.*, pp. 850–853, 2016.
- [34] M. Hirtz, A. Oikonomou, N. Clark, Y.-J. Kim, H. Fuchs, and A. Vijayaraghavan, "Self-limiting Multiplexed Assembly of Lipid Membranes on Large-area Graphene Sensor Arrays," *Nanoscale*, p. (to be submitted), 2015.
- [35] C. A. Keller and B. Kasemo, "Surface specific kinetics of lipid vesicle adsorption measured with a quartz crystal microbalance," *Biophys. J.*, vol. 75, no. 3, pp. 1397–1402, 1998.
- [36] N.-J. J. Cho, C. W. Frank, B. Kasemo, and F. Hook, "Quartz crystal microbalance with dissipation monitoring of supported lipid bilayers on various substrates," *Nat. Protoc.*, vol. 5, no. 6, pp. 1096–1106, May 2010.
- [37] E. Reimhult, F. Höök, and B. Kasemo, "Vesicle adsorption on SiO<sub>2</sub> and TiO<sub>2</sub>: Dependence on vesicle size," *J. Chem. Phys.*, vol. 117, no. 16, pp. 7401–7404, 2002.
- [38] R. P. Richter and A. R. Brisson, "Following the formation of supported lipid bilayers on mica: a study combining AFM, QCM-D, and ellipsometry," *Biophys. J.*, vol. 88, no. 5, pp. 3422–3433, 2005.
- [39] B. Seantier and B. Kasemo, "Influence of mono-and divalent ions on the formation of supported phospholipid bilayers via vesicle adsorption," *Langmuir*, vol. 25, no. 10, pp. 5767–5772, 2009.
- [40] M. Dacic, J. A. Jackman, S. Yorulmaz, V. P. Zhdanov, B. Kasemo, and N. J. Cho, "Influence of divalent cations on deformation and rupture of adsorbed lipid vesicles," *Langmuir*, vol. 32, no. 25, pp. 6486–6495, 2016.
- [41] J. T. Marquês, R. F. M. de Almeida, and A. S. Viana, "Biomimetic membrane rafts stably supported on unmodified gold," *Soft Matter*, vol. 8, p. 2007, 2012.
- [42] C. A. Keller, K. Glasmästar, V. P. Zhdanov, and B. Kasemo, "Formation of supported membranes from vesicles," *Phys. Rev. Lett.*, vol. 84, no. 23, p. 5443, 2000.
- [43] S. Kim and S.-J. Choi, "A lipid-based method for the preparation of a piezoelectric DNA biosensor," *Anal. Biochem.*, vol. 458, pp. 1–3, 2014.
- [44] M. Kasper, L. Traxler, J. Salopek, H. Grabmayr, A. Ebner, and F. Kienberger, "Broadband 120 MHz Impedance Quartz Crystal Microbalance (QCM) with Calibrated Resistance and Quantitative Dissipation for Biosensing Measurements at Higher Harmonic Frequencies," *Biosensors*, vol. 6, no. 2, p. 23, 2016.
- [45] R. Frost, G. E. Jo?nsson, D. Chakarov, S. Svedhem, and B. Kasemo, "Graphene oxide and lipid membranes: interactions and nanocomposite structures," *Nano Lett.*, vol. 12, no. 7, pp. 3356–3362, 2012.
- [46] M. Yang and J. He, "Graphene oxide as quartz crystal microbalance sensing layers for detection of formaldehyde," *Sensors Actuators B Chem.*, vol. 228, pp. 486–490, 2016.
- [47] J. Munro and C. Frank, "In Situ Formation and Characterization of Poly (ethylene glycol)-Supported Lipid Bilayers on Gold ...," *Langmuir*, no. 7, pp. 10567–10575, 2004.
- [48] J. Ekeröth, P. Konradsson, and F. Höök, "Bivalent-ion-mediated vesicle adsorption and controlled supported phospholipid bilayer formation on molecular phosphate and sulfate layers on gold," *Langmuir*, vol. 18, no. 21, pp. 7923–7929, 2002.
- [49] S. R. Tabaei, W. B. Ng, S.-J. Cho, and N.-J. Cho, "Controlling the Formation of Phospholipid Monolayer, Bilayer, and Intact Vesicle Layer on Graphene," *ACS Appl. Mater. Interfaces*, vol. 8, no. 18, pp. 11875–11880, 2016.
- [50] R. P. Richter, R. Bérat, and A. R. Brisson, "Formation of solid-supported lipid bilayers: An integrated view," *Langmuir*, vol. 22, no. 8, pp. 3497–3505, 2006.
- [51] R. Tero, H. Watanabe, and T. Urisu, "Supported phospholipid bilayer formation on hydrophilicity-controlled silicon dioxide surfaces," *Phys. Chem. Chem. Phys.*, vol. 8, no. 33, p. 3885, 2006.
- [52] G. Edward Gnana Jothi, S. Kamatchi, and a. Dhathathreyan, "Adsorption of DOPC vesicles on hydrophobic substrates in the presence of electrolytes: A QCM and reflectometry study," *J. Chem. Sci.*, vol. 122, no. 3, pp. 341–348, 2010.

- [53] S. Pei and H. Cheng, "The reduction of graphene oxide," *Carbon N. Y.*, vol. 50, no. 9, pp. 3210–3228, 2011.
- [54] H. Loughrey, M. B. Bally, and P. R. Cullis, "A non-covalent method of attaching antibodies to liposomes," *Biochim. Biophys. Acta (BBA)-Biomembranes*, vol. 901, no. 1, pp. 157–160, 1987.
- [55] R. P. Haugland and W. W. You, "Coupling of monoclonal antibodies with biotin," *Methods Mol. Biol.*, vol. 45, pp. 223–233, 1995.
- [56] D. Shetty, J. K. Khedkar, K. M. Park, and K. Kim, "Can we beat the biotin–avidin pair?: cucurbit [7] uril-based ultrahigh affinity host–guest complexes and their applications," *Chem. Soc. Rev.*, vol. 44, no. 23, pp. 8747–8761, 2015.
- [57] P. Vilja, K. Krohn, and P. Tuohimaa, "A rapid and sensitive non-competitive avidin-biotin assay for lactoferrin," *J. Immunol. Methods*, vol. 76, no. 1, pp. 73–83, 1985.
- [58] V. Singh, D. Joung, L. Zhai, S. Das, S. I. Khondaker, and S. Seal, "Graphene based materials: Past, present and future," *Prog. Mater. Sci.*, vol. 56, no. 8, pp. 1178–1271, 2011.
- [59] W. S. Hummers and R. E. Offeman, "Preparation of Graphitic Oxide," *J. Am. Chem. Soc.*, vol. 80, no. 6, p. 1339, 1958.
- [60] Marco Brugnara (marco.brugnara at ing.unitn.it), "Contact Angle Plugin," 2006. [Online]. Available: <https://imagej.nih.gov/ij/plugins/contact-angle.html>. [Accessed: 06-Oct-2017].
- [61] R. Richter, A. Mukhopadhyay, and A. Brisson, "Pathways of lipid vesicle deposition on solid surfaces: a combined QCM-D and AFM study," *Biophys. J.*, vol. 85, no. 5, pp. 3035–47, 2003.
- [62] T. Smith, "The hydrophilic nature of a clean gold surface," *J. Colloid Interface Sci.*, vol. 75, no. 1, pp. 51–55, 1980.
- [63] R. Woods and P. Melbourne, "The hydrophilic nature of gold and platinum," vol. 81, pp. 285–290, 1977.
- [64] M. Li, M. Chen, E. Sheepwash, C. L. Brosseau, H. Li, B. Pettinger, H. Gruler, and J. Lipkowski, "AFM Studies of Solid-Supported Lipid Bilayers Formed at a Au ( 111 ) Electrode Surface Using Vesicle Fusion and a Combination of Langmuir - Blodgett and Langmuir - Schaefer Techniques," no. 111, pp. 10313–10323, 2008.
- [65] N.-J. Cho, C. W. Frank, B. Kasemo, and F. Höök, "Quartz crystal microbalance with dissipation monitoring of supported lipid bilayers on various substrates," *Nat. Protoc.*, vol. 5, no. 6, pp. 1096–106, 2010.
- [66] I. Czolkos, A. Jesorka, and O. Orwar, "Molecular phospholipid films on solid supports," *Soft Matter*, vol. 7, no. 10, p. 4562, 2011.
- [67] N. Cho and C. W. Frank, "Fabrication of a Planar Zwitterionic Lipid Bilayer on Titanium Oxide," vol. 26, no. 14, pp. 15706–15710, 2010.
- [68] A. C.-F. Ip, B. Liu, P.-J. J. Huang, and J. Liu, "Oxidation Level-Dependent Zwitterionic Liposome Adsorption and Rupture by Graphene-based Materials and Light-Induced Content Release," *Small*, vol. 9, no. 7, pp. 1030–1035, 2013.
- [69] P.-J. J. J. Huang, F. Wang, and J. Liu, "Liposome/Graphene Oxide Interaction Studied by Isothermal Titration Calorimetry," *Langmuir*, vol. 32, no. 10, pp. 2458–2463, 2016.
- [70] W. N. U. A. V. AF, I. M, L. M, H. M, V. A, and S. MS, "Biomimetic Phospholipid Membrane Organization on Graphene and Graphene Oxide Surfaces: a Molecular Dynamics Simulation Study," 2017.
- [71] A. C.-F. Ip, B. Liu, P.-J. J. J. Huang, and J. Liu, "Oxidation Level-Dependent Zwitterionic Liposome Adsorption and Rupture by Graphene-based Materials and Light-Induced Content Release," *Small*, vol. 9, no. 7, pp. 1030–1035, 2013.
- [72] S. O. Rivel, Thimothée Yesylevskyy and C. Ramseyer, "Structures of single , double and triple layers of lipids adsorbed on graphene : Insights from all-atom molecular dynamics simulations," vol. 118, pp. 358–369, 2017.
- [73] Y. Okamoto, K. Tsuzuki, S. Iwasa, R. Ishikawa, a Sandhu, and R. Tero, "Fabrication of Supported Lipid Bilayer on Graphene Oxide," *J. Phys. Conf. Ser.*, vol. 352, p. 12017, 2012.
- [74] K. Furukawa and H. Hibino, "Self-spreading of Supported Lipid Bilayer on SiO<sub>2</sub> Surface Bearing Graphene Oxide," *Chem. Lett.*, vol. 41, no. 10, pp. 1259–1261, 2012.
- [75] R. Frost, S. Svedhem, C. Langhammer, and B. Kasemo, "Graphene Oxide and Lipid Membranes: Size-Dependent Interactions," *Langmuir*, vol. 32, no. 11, pp. 2708–2717, 2016.
- [76] M. Hirtz, A. Oikonomou, T. Georgiou, H. Fuchs, and A. Vijayaraghavan, "Multiplexed biomimetic lipid membranes on graphene by dip-pen nanolithography," no. May, 2013.
- [77] O. C. Compton and S. T. Nguyen, "Graphene Oxide, Highly Reduced Graphene Oxide, and Graphene: Versatile Building Blocks for Carbon-Based Materials," *small*, vol. 6, no. 6, pp. 711–723, 2010.
- [78] K. Yamazaki, S. Kunii, and T. Ogino, "Characterization of interfaces between graphene films and support substrates by observation of lipid membrane formation," *J. Phys. Chem. C*, vol. 117, no. 37, pp. 18913–18918, 2013.
- [79] M. Hirtz, A. Oikonomou, T. Georgiou, H. Fuchs, and A. Vijayaraghavan, "DPN116-Multiplexed biomimetic lipid membranes on graphene by dip-pen nanolithography," *Nat. Commun.*, vol. 4, no. May, p. 2591, 2013.
- [80] J. Rafiee, X. Mi, H. Gullapalli, A. V. Thomas, F. Yavari, Y. Shi, P. M. Ajayan, and N. A. Koratkar, "Wetting transparency of graphene," *Nat. Mater.*, vol. 11, no. 3, pp. 217–222, 2012.
- [81] E. Sackmann, "Supported membranes: Scientific and practical applications," *Science (80-. )*, vol. 271, no. 5245, pp. 43–48, 2007.
- [82] M. Eeman and M. Deleu, "From biological membranes to biomimetic model membranes," *Biotechnol. Agron. Soc. Environ.*, vol. 14, no. 4, pp. 719–736, 2010.
- [83] R. Maget-Dana, *The monolayer technique: A potent tool for studying the interfacial properties of antimicrobial and membrane-lytic peptides and their interactions with lipid membranes*, vol. 1462, no. 1–2. 1999.